JOURNAL OF GEOPHYSICAL RESEARCH, VOL. 106, NO. E12, PAGES 33,005-33,020, DECEMBER 25,2001

Paterae on Io: A new type of volcanic caldera?

Jani Radebaugh, Laszlo P. Keszthelyi, Alfred S. McEwen, Elizabeth P. Turtle,
Windy Jaeger, and Moses Milazzo

Lunar and Planetary Laboratory, University of Arizona, Tucson, Arizona

Abstract. Paterae, defined by the International Astronomical Union as "irregular crater[s], or complex one[s] with scalloped edges," are some of the most prominent topographic features on Io. Paterae on Io are unique, yet in some aspects they resemble calderas known and studied on Earth, Mars, and Venus. They have steep walls, flat floors, and arcuate margins and sometimes exhibit nesting, all typical of terrestrial and Martian basalt shield calderas. However, they are much larger, many are irregular in shape, and they typically lack shields. Their great sizes (some >200 km diameter) and lack of associated volcanic edifices beg comparison with terrestrial ash flow calderas; however, there is no convincing evidence on Io for the high-silica erupted products or dome resurgence associated with this type of caldera. Ionian paterae seem to be linked with the eruption of large amounts of mafic to ultramafic lavas and colorful sulfur-rich materials that cover the floors and sometimes flow great distances away from patera margins. They are often angular in shape or are found adjacent to mountains or plateaus, indicating tectonic influences on their formation. A database of 417 paterae on Io measured from images with <3.2 km pixel^{-1} resolution (80% of its surface) reveals that their mean diameter of 41.0 km is close to that for calderas of Mars (47.7 km), is smaller than that for Venus (~68 km), but dwarfs those for terrestrial basalt shield calderas (6.6 km) and ash flow calderas (18.7 km). Thirteen percent of all paterae are found adjacent to mountains, 42% have straight or irregular margins, and 8% are found atop low shields. Abundant, smaller paterae with more continuously active lava eruptions are found between 25 S and 25 N latitude, whereas fewer and larger paterae are found poleward of these latitudes. Patera distribution shows peaks at 330 W and 150 W longitude, likely related to the direction of greatest tidal massaging by Jupiter. Ionian patera formation may be explained by portions or combinations of models considered for formation of terrestrial calderas, yet their unusual characteristics may require new models with a greater role for tectonic processes.

1. Introduction

Jupiter's moon Io is a body replete with amazing geologic features, such as giant lava flows, high lava fountains, and tall mountains. Among the most prominent and significant of these features are the paterae: saucer-like depressions that are often filled with lava flow deposits. The International Astronomical Union definition of patera is "an irregular crater, or a complex one with scalloped edges" (Planetary Nomenclature home page, http://wwwflag.wr.usgs.gov/USGSFlag/Space/nomen/nomen.html, 2000). This definition does not make assumptions about formation mechanism or whether or not paterae have a volcanic or any other genetic association, except that they lack the obvious characteristics of well-preserved impact craters. Ionian paterae do not appear to be lunar-type lava-filled impact basins; their morphologies and size-frequency distributions are different.

Paterae found on Io have mostly been interpreted to be volcanic calderas [*Carr et al.*, 1979; *Schaber*, 1982; *McEwen et al.*, 1985], similar to those found on Earth, Mars, and Venus, all planets on which there has been vigorous and long-lived volcanism. A terrestrial caldera is defined as a large volcanic depression, more or less circular in form, the diameter of which is many times greater than any included vent [*Williams*, 1941]. Because of the unique characteristics of calderas on other planets, *Wood* [1984, p. 8405] suggested the definition "a multi-kilometer wide, quasi-circular depression, not of impact origin, formed in volcanic terrain by collapse into a partially drained magma chamber." He added that "calderas occur in volcanic systems which are repeatedly active over long time periods (10^3-10^6 years)," to distinguish them from volcanic craters. Unfortunately, on Io it is difficult to confirm that paterae form primarily by collapse due to the draining of a shallow magma chamber, making us cautious in applying the term "caldera" to

Paper number 2000JE001406.
0148-0227/01/2000JE001406$09.00

paterae. We describe Ionian paterae and then discuss mechanisms for their formation.

Io is currently the most volcanically active body in the solar system, and it is possible to watch changes associated with many of its over 400 paterae. We have observed color and albedo changes at Pillan, Prometheus, and many other paterae over 20 years [*McEwen et al.*, 1998a]. In addition, some paterae's colors or albedos have changed between Galileo spacecraft orbits, such as Tvashtar Catena (a string of paterae) and Pillan Patera [*Phillips*, 2000]. Images of Io's surface acquired by Galileo do not reveal changes to patera topography.

Thermal observations indicate that most or all dark areas on Io are currently, or were very recently, active [*McEwen et al.*, 1985, 1997]. The majority of paterae on Io (83% of those measured at <3.2 km pixel^{-1} resolution) have floors that are partially or completely dark (normal reflectance < 0.4), but many are potentially mantled with high-albedo material, possibly SO_2 frost from nearby eruptions [*Geissler, et al.*, 1999] (Plate 1). These ghost paterae did not have active lava flows associated with them in the recent past, yet they must be young features, given that the global average age of Io's surface is < 1 million years old [*Johnson and Soderblom*, 1982; *Phillips*, 2000]. A volcanic body on Earth is active if it has erupted in historic times, or dormant if it is not erupting but likely to do so in the future [*Jackson*, 1997]. By these standards, volcanic eruptions within most of the >400 paterae seen on the young surface of Io may be active or dormant.

First we discuss observations of the appearance and behavior of paterae on Io, derived from images obtained by Galileo and Voyager spacecraft. We compiled a new database recording information for all paterae on Io imaged at <3.2 km pixel^{-1} resolution. This database was created to find global interrelationships between Ionian paterae. Following discussion of database statistics, specific descriptions of paterae are recorded, with reference to their tectonic associations, locations on Io, and associated lava flow features. Implications of the analyses of patera morphologies are then addressed, through comparisons with calderas on Earth, Mars, and Venus. Our broad base of knowledge about calderas on these other planets allows comparisons with paterae of Io, for which we have relatively new and limited information. Finally, we discuss conditions in Io's interior and possible models for patera formation.

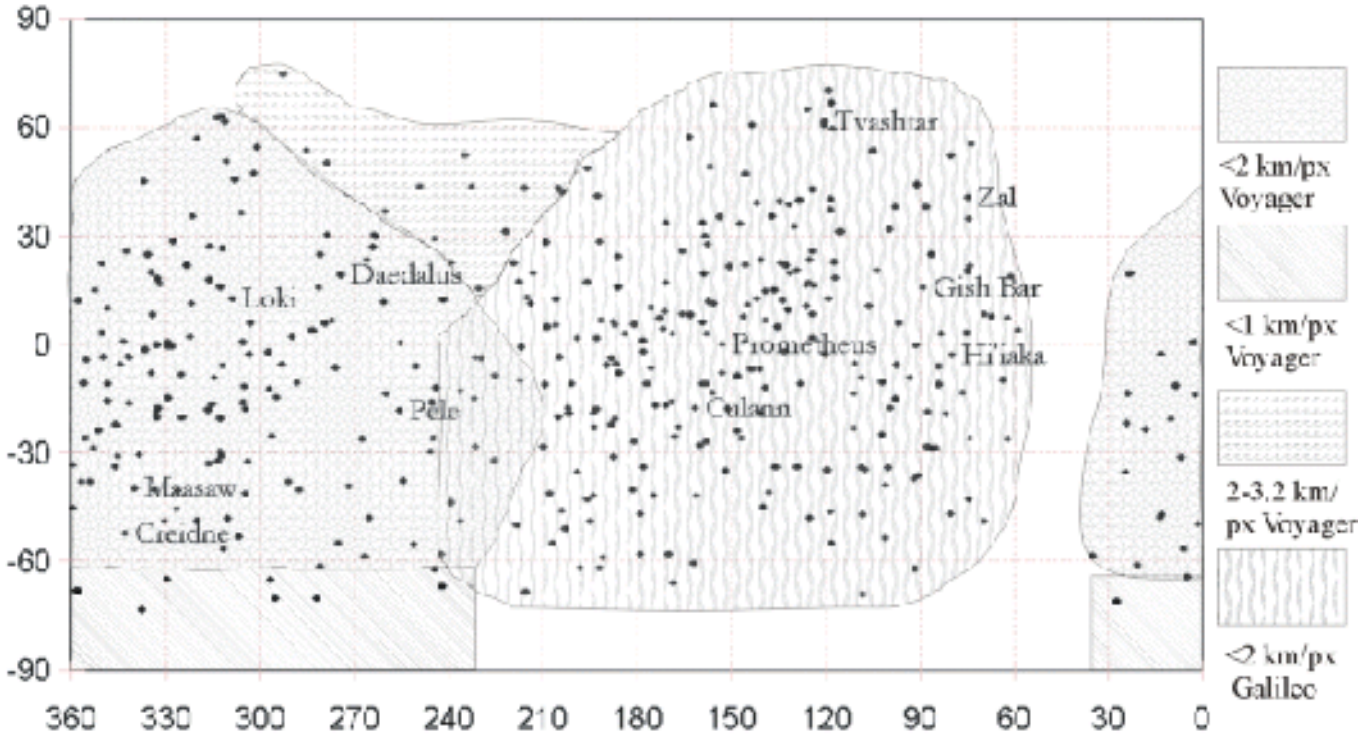

Figure 1. Map of locations of Ionian paterae overlain by image resolutions in regions imaged by Galileo and Voyager. About 80% of the planet has been imaged at resolutions of 3.2 km pixel^{-1} or better (the majority of that at <2 km pixel^{-1}). Boundaries are approximate. Voyager resolutions from *Schaber* [1982] and USGS Io maps.

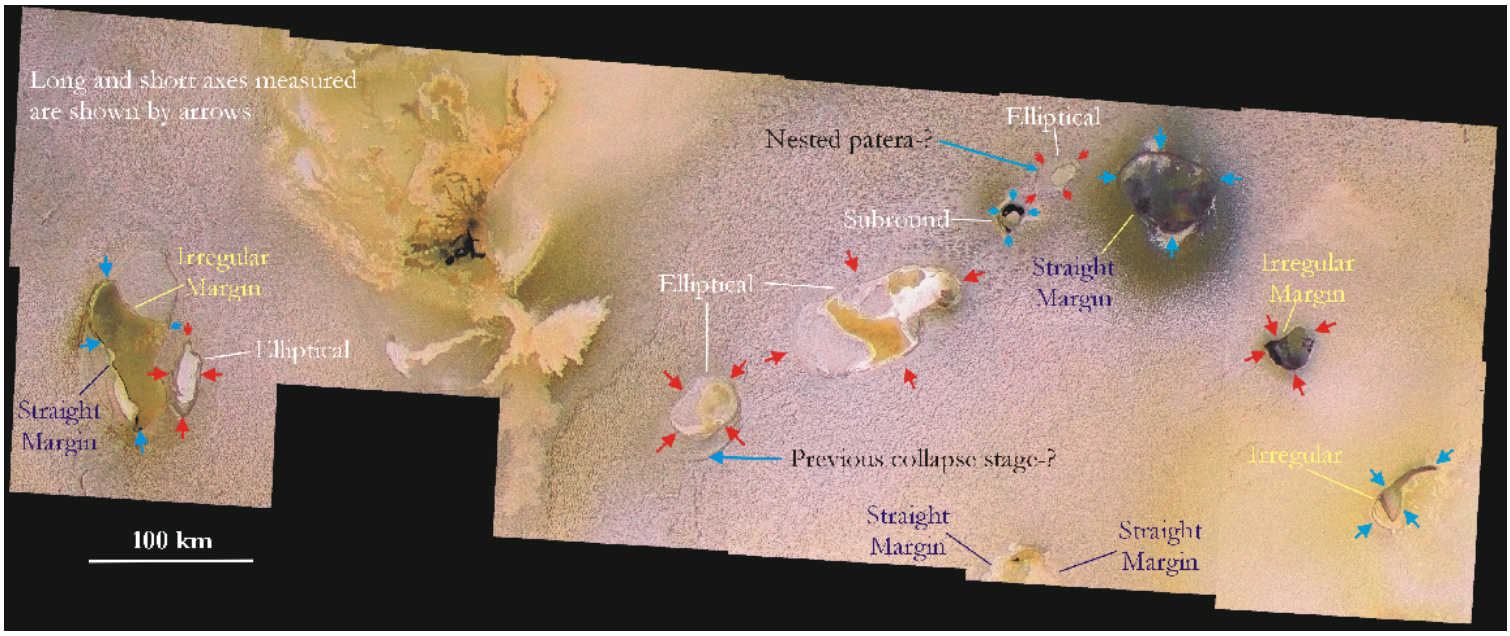

Plate 1. A string of Ionian paterae; there are 12 shown in this image, ranging from <5 km to over 90 km long axis (Chassc Patera, west end of image). Long and short axes are marked with arrows. Paterae with irregular and/or straight margins are labeled; paterae labeled elliptical, subround, and round are considered regular. The range of colors displayed within and around the paterae is likely due to the presence of SO2 and elemental S. Camaxtli Patera (east end of image) has a floor mottled by recent flows and is surrounded by dark diffuse material, possibly silicate pyroclastics. The small dark patera west of Camaxtli is a source of high heat output observed by NIMS in October 1999. Image taken by Galileo SSI February 2000 at 200 m/pixel resolution; image covers 130 W to 160 W longitude, 10 N latitude, 850 km across.

Table 1. Summary of Statistical Analyses of Patera/Caldera Diameters and Distributionsa

Category	nb	Maximumc	Mean	Median	SD	Kurtosis	Skew	Adjacent to Mountain	Irregular/ Straight Sides	Atop Shield
Io										
All	417	202.6	41.0	34.5	30.6	4.2	1.6	54	173	35
25 S -25 N	224	202.6	38.0	32.4	27.3	5.6	1.7			
25-90 S, 25-90 N	193	198.6	44.6	38.6	33.8	3.0	1.5			
Sub- 315-45 W	90	115.3	34.7	30.7	26.7	1.0	1.1			
Anti- 135-225 W	135	166.0	35.9	33	22.8	8.1	2			
Leading 45-135 W	99	161.6	43.7	35.5	30.5	1.7	1.1			
Trailing 225-315 W	93	202.6	52.0	48.7	39.9	2.7	1.3			
Earth										
Ash flow	129	76.9	18.7	15.4	12.4	6.3	2.2	N/A	N/A	0
Basalt shield	43	18.5	6.6	5.3	4.9	-0.1	0.9	0	N/A	43
Mars	37	145.0	47.7	39	35.8	0.3	0.9	0	7	36
Venusd	88	~200	~68	~70	~33.2	~1.6	~1.1	N/A	N/A	N/A

a N/A indicates not available.

b Number of paterae/calderas.

c All diameters given in km.

d Venus statistics approximate; data incomplete.

2. Catalog of Io Paterae

A new database of Ionian paterae records their sizes, distributions with latitude and longitude, morphological characteristics, proximity to mountains, straightness or irregularity of margins, and presence atop shields. The resolution of the images used was restricted to 3.2 km pixel^{-1}, although it is 1-2 km pixel^{-1} for most regions. Information was obtained from both Galileo and Voyager spacecraft missions as they have best imaged different hemispheres of the moon. Approximately 80% of the moon's surface has been imaged at this resolution (Figure 1); in this area 417 paterae have been catalogued. If we extrapolate the number of paterae on this fraction of Io to a number of paterae on the total surface area, we estimate that close to 500 paterae cover the surface of Io (accounting for more sparse distribution near the poles), higher than was previously expected [*Carr et al.*, 1979]. Paterae with faint outlines, which appeared to have been covered, were included in the catalog, but there may be many older, filled, barely recognizable paterae that were not measured.

2.1. Patera Sizes

Sizes of all 417 paterae were determined by measuring their long and short axes. The area of an ellipse containing the axes was calculated, and the effective diameter of the patera was defined as the diameter of a circle having the same area as the ellipse. For irregular features the dimensions measured are as representative as possible of the area of the patera. The minimum and maximum diameters measured are 2.5 and 202.6 km, and many are quite large, as 292 of the features measured have >20 km diameters. Measurements of paterae and assessment of characteristics were done using images from ~1 to 2 km pixel^{-1}, where possible, to maintain consistency across the database. There is one region from ~200 W to 270 W and ~30 N to 60 N imaged by Voyager with resolution of 2.0-3.2 km pixel^{-1} in which paterae were measured. Voyager also imaged half of the south polar region, from ~240 W to 20 W and ~60 S to 90 S, at <1 km pixel^{-1} (Figure 1). Several regions have high resolution Galileo images that overlap the ~2 km pixel^{-1} images, most commonly at ~200 m pixel^{-1}, but up to ~7 m pixel^{-1}, and these were also analyzed for the presence of paterae. On the basis of these high resolution images, we have concluded that the surface is not littered with small-sized features (<~10 km diameter), interspersed with fewer and larger features, as is seen in impact crater distributions (see Plate 1).

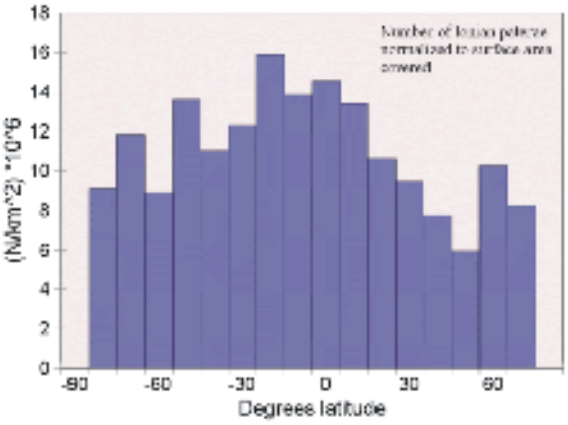

Figure 3. Histogram of 417 Ionian paterae versus degrees latitude, normalized to area covered. Greater numbers of paterae are found at equator-flanking latitudes, between 25 S and 25 N, than poleward of these latitudes.

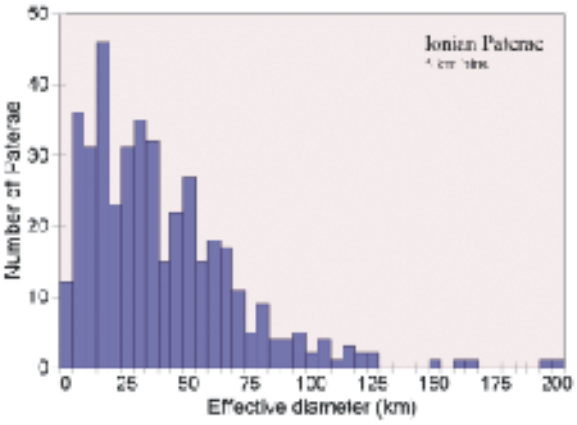

Figure 2. Histogram of 417 Ionian paterae measured at 3.2 km pixel^{-1} resolution or better versus effective diameter. Minimum is 2.5 km, maximum is 202.6 km diameter, and mean is 41.0 km diameter. A peak in distribution occurs between 15 and 20 km diameter, numbers then taper off exponentially to higher diameters.

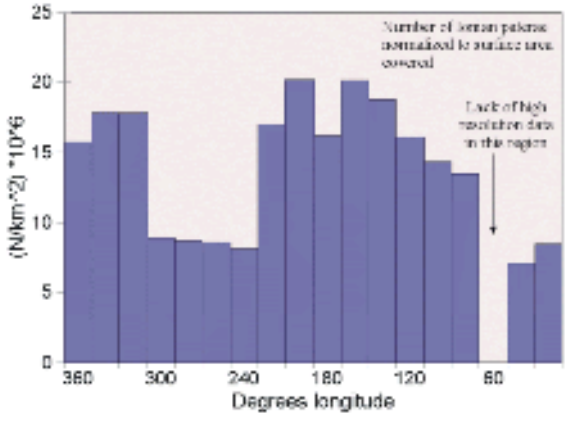

Figure 4. Histogram of 417 Ionian paterae versus degrees west longitude, normalized to area covered. Peaks in distribution occur at approximately 150 W and 330 W. The region from 200 W to 270 W and above 30 N (~25% of area measured at these longitudes) is at 1.2 km pixel^{-1} lower resolution than the majority of the rest of the planet.

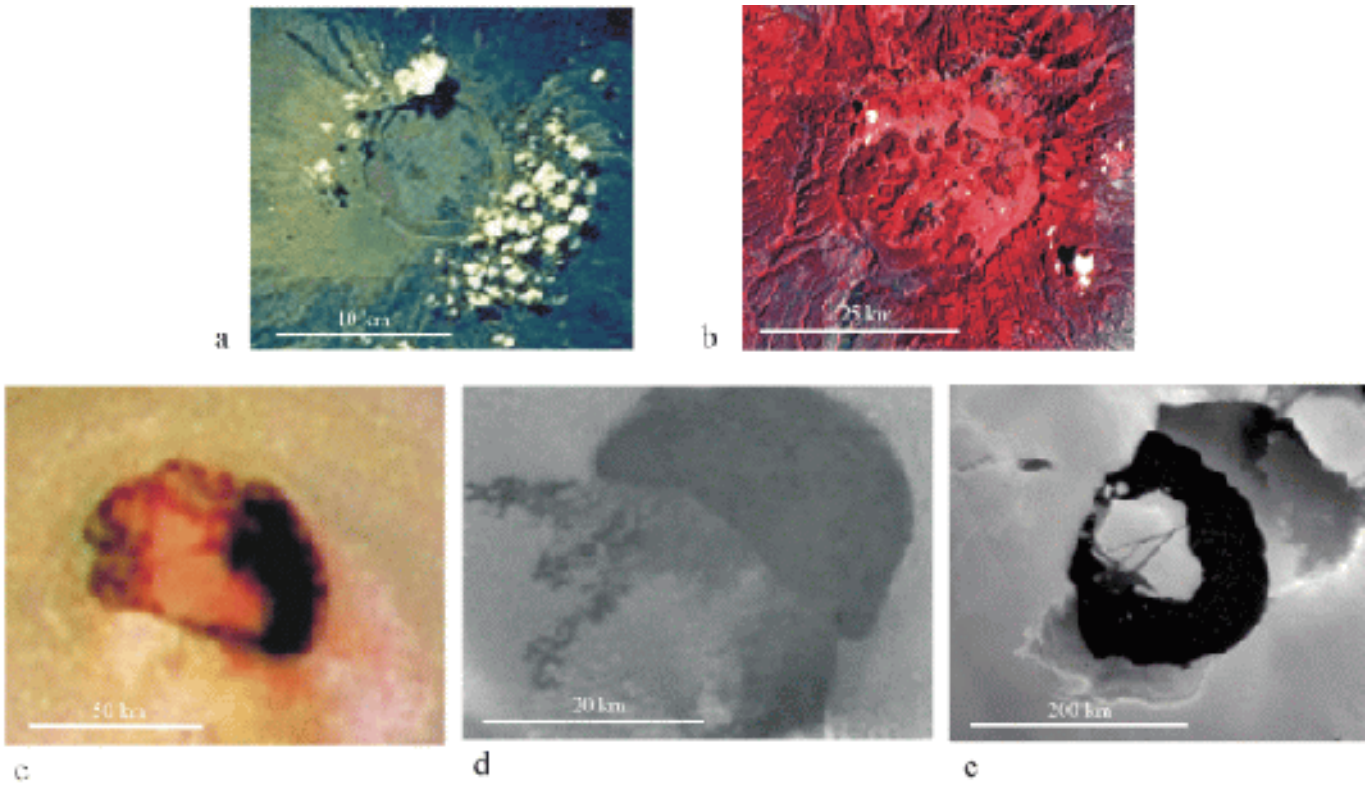

Figure 5. Two terrestrial calderas (top) shown next to three Ionian paterae for comparison (scales are all different). (a) A basalt shield caldera atop Isabela volcano, the Galapagos Islands; (b) Valles ash flow caldera, New Mexico; (c) Tupan Patera, (20 S, 140 W); (d) Prometheus Patera, (0 , 150 W); and (e) Loki Patera, (10 N, 310 W). Io images taken by Galileo or Voyager (Loki), Isabela SRL-1 image, taken on STS 059-213-019, courtesy of NASA, and Valles Landsat image courtesy of LANL/NASA.

Thus there may be a lower limit to the size at which these features tend to form. The mean diameter of the distribution of all paterae is 41.0 km and the median is 34.5 (Figure 2 and Table 1). Standard deviation is 30.6, indicating a broad spread in data, and similarly there is a leptokurtic kurtosis of +4.2, meaning the distribution has fatter tails than in a normal distribution. Distribution of data is positively skewed (+1.6) to the right. Data do not follow a normal distribution; rather, there is a concentration of features at 15-20 km diameter (and fewer at diameters <15 km) and then an exponential decline in number toward higher diameters.

2.2. Distribution With Latitude/Longitude

Paterae in the database are identified by their locations on the basis of the latitude and longitude of the intersection of their axes. Most observed paterae on Io exist between -25 and +25 latitude; their numbers over a given area are smaller poleward of this band. Figure 3 is a graph of latitudinal bands versus numbers of Ionian paterae, normalized to surface area covered. Equal numbers across the histogram would indicate an even distribution, but this shows there are more paterae found at low latitudes. A few spikes in number occur at high latitudes, these may exist because image targeting was biased toward finding interesting features, such as paterae. In general, however, the numbers of paterae decline toward the poles. In addition, paterae from -25 to +25 latitude are slightly smaller than those at the poles. The mean diameter for paterae from -25 to +25 is 38.0 km, compared with a mean diameter poleward of these latitudes of 44.6 km. As with total patera data, standard deviations for these data are quite large, 27.3 km for equatorial regions and 33.8 km for high latitudes (Table 1). (The difference in means would increase if Loki (220 km long axis) was removed from the equatorial data set.)

There is also an uneven distribution of paterae with longitude. Figure 4 shows longitudinal bands versus number of paterae normalized to surface area covered. There is a gap in moderate resolution coverage (better than 3 km per pixel)

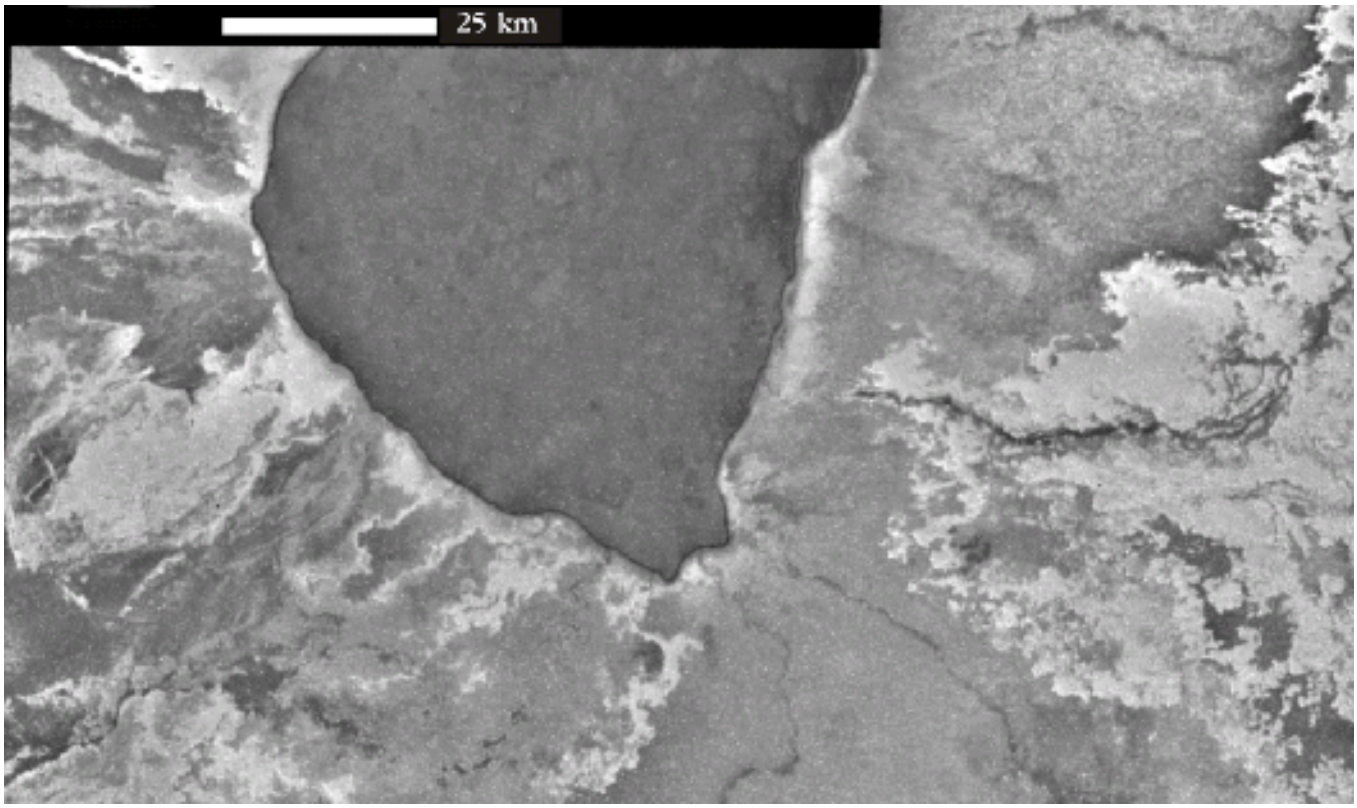

Figure 6. Close-up view of 80 km (long axis) Emakong Patera. Its dark floor indicates recent flows inside the patera, long dark flows radiate away from its walls. Some light flows emerge from the east edge of the patera, may be elemental sulfur flows. The patera is straight-sided, evidencing tectonic controls on its formation. Image by Galileo, November 1999, 150 m pixel^{-1} resolution.

between 40 W and 70 W longitude, and the region north of 30 from 200 W to 270 W is at a resolution of 2.0-3.2 km pixel^{-1}, instead of 1-2 km pixel^{-1} for other regions. However, normalized data show definite peaks in patera number occurring near 330 W and 150 W longitude, near the sub-Jovian and anti-Jovian points.. In addition, mean diameters of paterae are greater near longitudes 90 W and 270 W, at the leading and trailing quarters (43.7 and 52.0 km) of Io, than the sub-Jovian and anti-Jovian quarters (34.7 and 35.9 km). Hence paterae are less abundant but larger both at high latitudes and leading and trailing equatorial regions. Additional statistics for this analysis are listed in Table 1.

2.3 Association Between Paterae and Tectonic Features

The planform shapes of Ionian paterae range from round to extremely angular. Of 417 paterae measured at <2 km pixel^{-1} resolution, 42% have irregular margins or straight sides that terminate at sharp corners. Five of the paterae in Plate 1 are classified as irregular, or having oddly curved, sharply bent, or straight-sided margins, based on visual interpretation of images. Tupan, Prometheus, Loki (Figures 5c, 5d, and 5e) and Emakong (Figure 6) Paterae are all examples of features with straight margins ending at sharp corners. All paterae that are round, subround, or elliptical with smooth, continuous margins are considered to be regular, as are five of the paterae in Plate 1. The ellipticity of all paterae is determined on the basis of the ratio of their long to short axes. Ellipticity of paterae in this database ranges from 1 (equivalent axes) to 5.73. Seventy percent of paterae have ellipticites >1.25. This is only a way to quantify ratio of axes, however, and does not take into account margin morphologies; so elliptical does not equal irregular.

Shadow measurements from near-terminator images of paterae reveal very deep floors and steep walls [*Carr and Clow*, 1984]. High-resolution images (7-8 m pixel^{-1}) obtained by Galileo in February 2000 during the I27 orbit show the region within and around Chaac Patera (Figure 7). A shadow cast on the patera wall and floor enabled calculation of the height and slope of the wall; it was found to be 2.7 km high, with a 70 slope. For comparison, the deepest section of the Grand Canyon, Arizona, is ~1.5 km rim to river. While the upper, more resistant layers have comparably steep slopes, the whole sequence taken together (at Yuma Point, Arizona) has a slope of only 30 . To create walls of the dimensions of

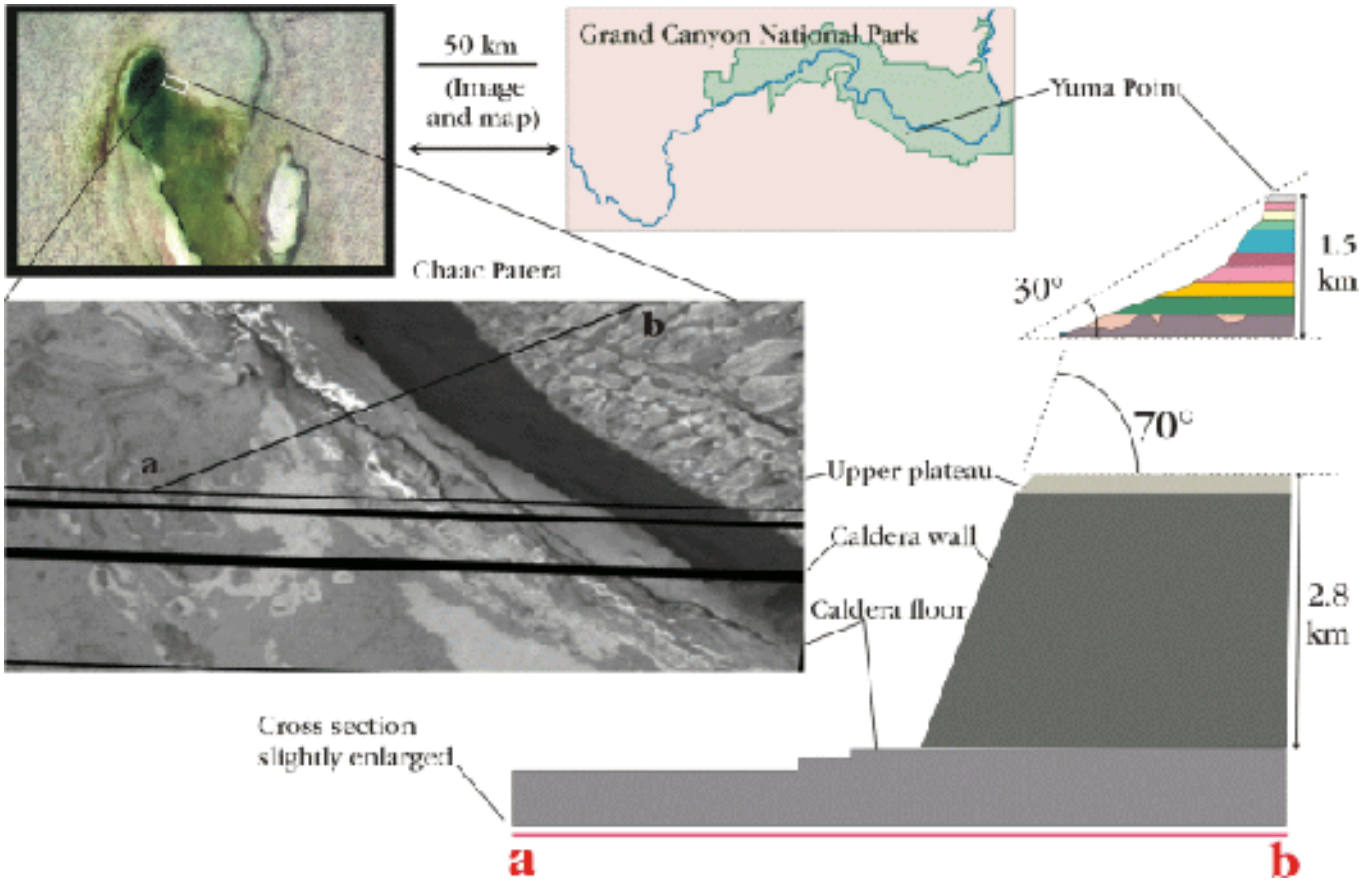

Figure 7. Chaac Patera and a cross-section of its wall shown with the Grand Canyon for comparison. Io images by Galileo, February 2000, top image is 200 m pixel^{-1}, bottom is 7-8 m pixel^{-1}. Grand Canyon cross section from Geologic Map of the Grand Canyon, by G. Billingsly et al.

Chaac Patera requires a tremendous amount of movement within the upper lithosphere of Io. The walls of Chaac, and possibly all other paterae (and mountains), must be made of materials strong enough to support such steep slopes without disintegrating by immediate mass wasting [*Carr et al.*, 1979; *Carr and Clow*, 1984].

Paterae on Io are sometimes adjacent to mountains. Mountains on Io are not volcanic in origin, but they appear to instead be tilted crustal blocks or stepped plateaus [*Turtle et al.*, this issue; *Schenk et al.*, this issue]. Of 417 paterae catalogued at <3.2 km pixel^{-1}, 13% can be seen to abut mountains or plateaus. This number is likely a lower limit, since it is difficult to discern mountains in low phase angle images except when stereo pairs are available (see Figure 10 of *Turtle et al.*, this issue). In comparison, *Jaeger et al.* [2001] determined that 42% of all mountains have one or more paterae adjacent to them. Paterae that abut mountains or plateaus are often oddly shaped, with arcuate or scalloped margins [*Carr et al.*, 1979], such as the clover-shaped Gish Bar Patera (Figure 8). This feature formed adjacent to a mountain, which is seen rising to the north of the patera margin. The mountain casts a shadow that can be traced down into the patera, revealing a steep wall that drops off to a deep, flat floor. Figure 9 shows Monan Patera and another patera at the north and south ends, respectively, of an elongate mountain. Monan has apparently formed around the mountain, creating an unusual worm-shaped depression.

We conclude that >40% of paterae show strong influences of regional tectonics. At high resolution (200-300 m pixel^{-1}), this becomes apparent on a detailed level. At Hi iaka Patera, a mountain appears dissected, separated by a rifted basin that has subsequently filled in with lava [see *Jaeger et al.*, 2001; *Turtle et al.*, this issue]. Zal, Shamash, and Monan Paterae also likely had a large degree of tectonic influence on their formation. Zal is an extremely large (197 km long axis), low feature which is bordered by plateaus on the east and west and a mountain to the south, with no definite northern margin (Figure 10). Dark lavas flow from fractures near the base of the walls across the floor, and the rest of the floor is green and brown, of a different texture than its surroundings. Shamash is 204 km along its long axis, has varicolored lavas on the floor, and is bordered by a mountain and a plateau. It has an irregular margin (where it

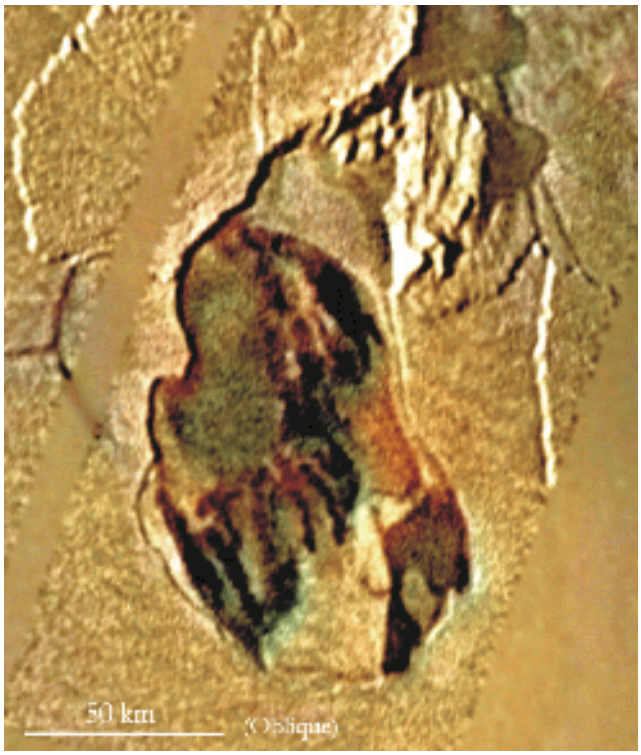

Figure 8. Slightly oblique view of Gish Bar Patera (15 N, 90 W). It is a large (106x115 km), irregular feature that may have formed as a result of several separate caldera collapses. Mottled lava flows cover any preexisting walls or floor characteristics. The caldera walls are steep; shadows can be traced from the mountain to the north down into the floor. Image taken by Galileo, 500 m pixel^{-1} resolution.

can be discerned), likely due to its mountain and plateau associations. The top and bottom margins of Monan (Figure 9) are congruent and almost appear to have been pulled apart from each other, away from the north end of the mountain.

2.4. High-Latitude Paterae

Paterae that form at high latitudes (>50 north or south) are often especially large and have some morphological differences from those at low latitudes. For example, a couple of features in the string of paterae called Tvashtar Catena (Figure 11) at 60-65 N, 118-126 W have dimensions of 177.5 x 80.6 km and 149.3 x 103.9 km. There are at least 10 large paterae in the south polar region, imaged by Voyager, from ~330 W to 35 W up to ~50 S that are separated by a few hundred kilometers with no other paterae between them. Creidne Patera at 52.4 S, 343.2 W is 169.9 x 78.2 km, Nusku Patera at 64.4 S, 4.9 W is 119.9 x 54.4 km, and Kane Patera at 47.8 S, 13.4 W is

Figure 9. Monan Patera (20 N, 105 W) is an elongate, 136-km-long feature; its similar north and south margins indicate that it may have formed as a pull-apart basin and subsequently filled in with lava. It borders the north edge of a mountain, and another large, straight-sided patera borders the south end of the same mountain. Image taken by Galileo, October 1999, 500 m pixel^{-1} resolution.

144.4 x 77.6 km. Compare the features in Figure 12, a Voyager mosaic, with typical low-latitude paterae seen in Plate 1. These high-latitude paterae often have margins that are steeper and more circular than paterae in regions

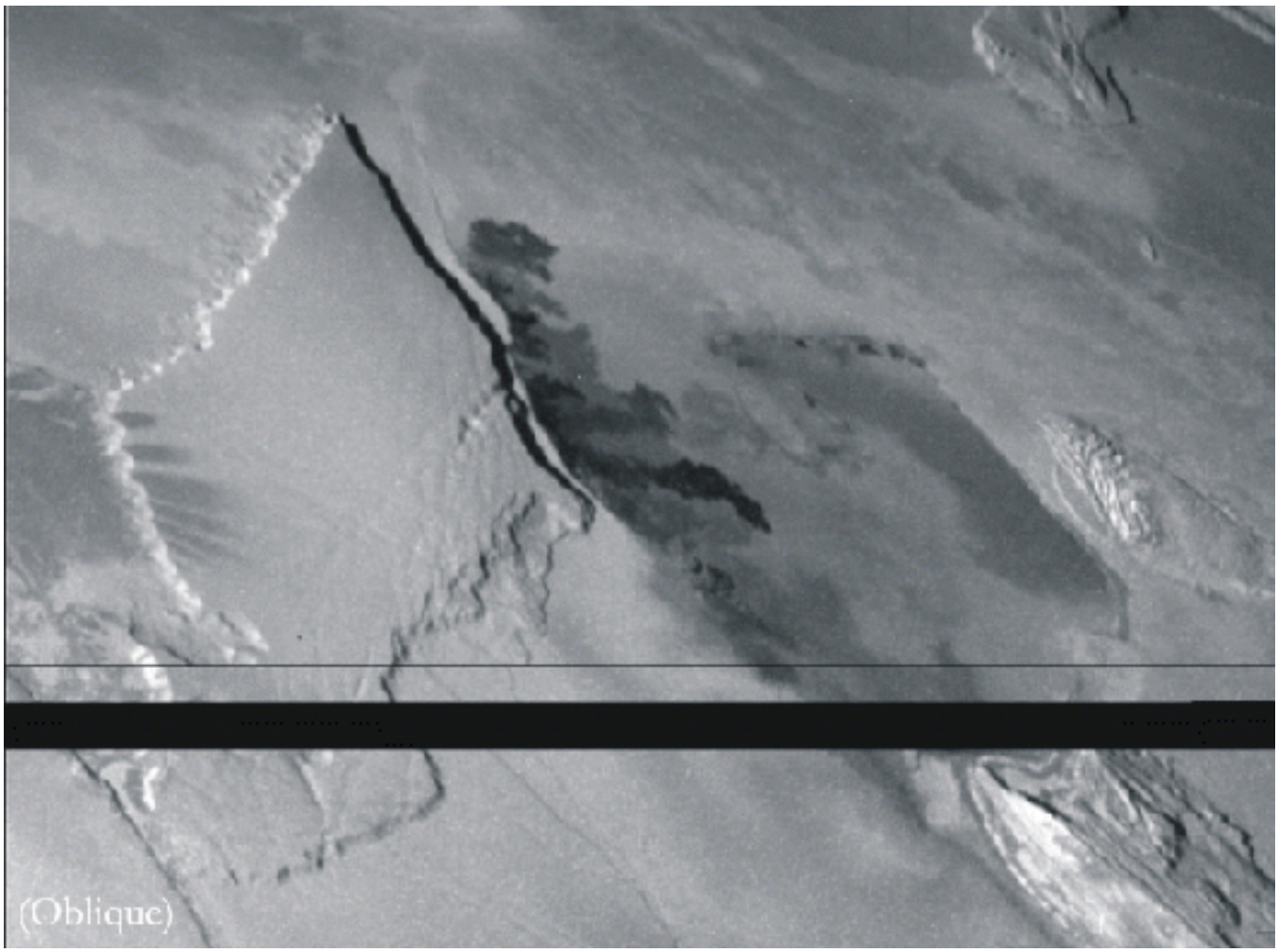

Figure 10. Oblique image of Zal Patera (40 N, 75 W). This is a large (198x132 km) depression surrounded on the west by a plateau and on the south and east by mountains, with no definite northern margin. Dark flows emerge into the patera from the west and east walls. Image taken by Galileo, February 2000, 335 m pixel^{-1} resolution.

flanking the equator, and they do not have extensive dark lava flow mottling as is seen on the floors of low-latitude paterae.

2.5. Paterae on Shields

It has generally been thought that Ionian paterae are missing shield edifices [*Schaber*, 1982]. Of the 80% of Io s surface that has been imaged at resolutions of 3.2 km pixel^{-1} or better, only 8% of all paterae measured have evidence of being associated with low shields. This is based either on the paterae being the source of long flows radiating in all directions, indicating topographic highs, or on the paterae sitting atop small features that have discernable basal scarps. It is important to keep in mind that broad, gently sloping features are very difficult to detect at low phase angle. A feature described by *Moore et al.* [1986] is a shield 75 by 90 km at the base, with a gentle slope, and a summit caldera 5 km across and 100 m deep. Two features at 10-20 S and 350 W, Apis and Inachus Tholi, are round, with positive scarps at the base, and they slope upward to small summit paterae. It is possible that additional paterae rest atop low shields that have not yet been detected.

2.6. Flows and Floor Mottling

No one type of erupted material is dominant in all Ionian paterae, so various characteristics of flows and deposits are discussed as specific examples. Dark lavas associated with ionian paterae appear to be mafic or ultramafic in composition [*McEwen et al.*, 1998a, 1998b]. They have reflectance <10% when fresh, are fluidly emplaced onto the patera floor, and in some cases extend away from the margins for hundreds of kilometers. Many of the flows that cover the floors of patera e, for example, in

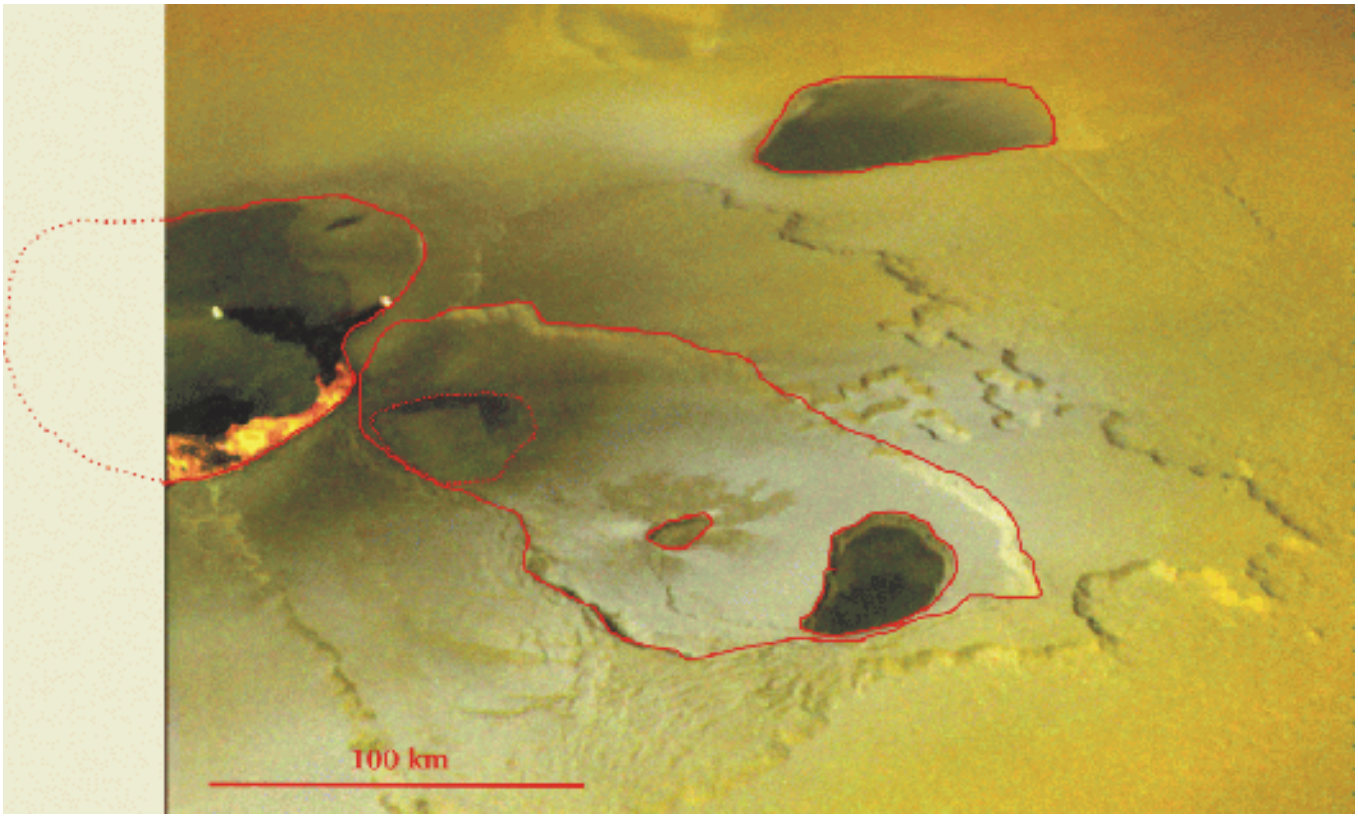

Figure 11. Slightly oblique view of Tvashtar Catena and outlines of separately measured paterae in this vicinity. Uncertain patera boundaries are dotted. Active lava flows are emerging from the base of the walls onto the floor of the far western patera. Image taken by Galileo, February 2000, 300 m pixel^{-1} resolution.

Chaac Patera, seem to be ponded with an inflated pahoehoe surface texture [*Keszthelyi et al.*, this issue]. Dark, tendril-like flows have emerged from a patera in the center left in Plate 1. Another example, Emakong, is a dark-floored patera that measures 80 km in diameter along its longest axis (Figure 6). Voluminous, fluid lava flows emerge from the patera walls and flow away from the patera for over 100 km. Another feature, the 30-km-diameter dark-floored patera associated with the Prometheus lava flow, also shows evidence of at least three separate lava flows emerging from its southwest margin (Figure 5d). There is a large ~100-km-long flow connected to the patera that culminates in the base of the large Prometheus plume; however it is not likely that this flow comes directly from the patera itself, but rather it comes from a vent several kilometers south of Prometheus Patera [*McEwen et al.*, 2000; *Lopes-Gautier et al.*, 2000].

Camaxtli Patera and a small feature to its west also exhibit extensive dark flows on their floors (Plate 1). Camaxtli has a dark rim, possibly because lava is erupted along the faults at the base of the patera walls, and has mottled dark flows and green deposits on its floor. The small patera to the west has an extremely dark floor and is the location of a strong hot spot seen by Near Infrared Mapping Spectrometer (NIMS) during the I24 Galileo flyby (October 1999) [*Lopes-Gautier et al.*, 2000]. Both dark paterae have diffuse white deposits on their floors and at their margins, as well as diffuse dark halos around them.

In addition to the dark lavas we often see light colored, fluid lavas emerging onto some patera floors and extending outward from their margins. Emakong Patera (Figure 6) has erupted light colored material from its east margin into a flow field hundreds of square kilometers in area that could possibly be composed of sulfur or sulfur compounds [*Williams et al.*, this issue]. A light colored, lobate tail over 100 km long emerges from what is possibly a small, dark patera in Plate 1 and appears to be covered by brighter colored flows in a butterfly-shaped pattern.

Patera floors are also often covered in white material, possibly SO_2 frost that accumulates in cooler, less active regions, such as the floor of the patera east of Chaac (Figure 7). NIMS confirmed the presence of SO_2 on the island of Loki [*Lopes-Gautier et al.*, 2000]. Often there are also coatings of yellow, orange, brown, and bright green units, all thought to be elemental sulfur allotropes, perhaps

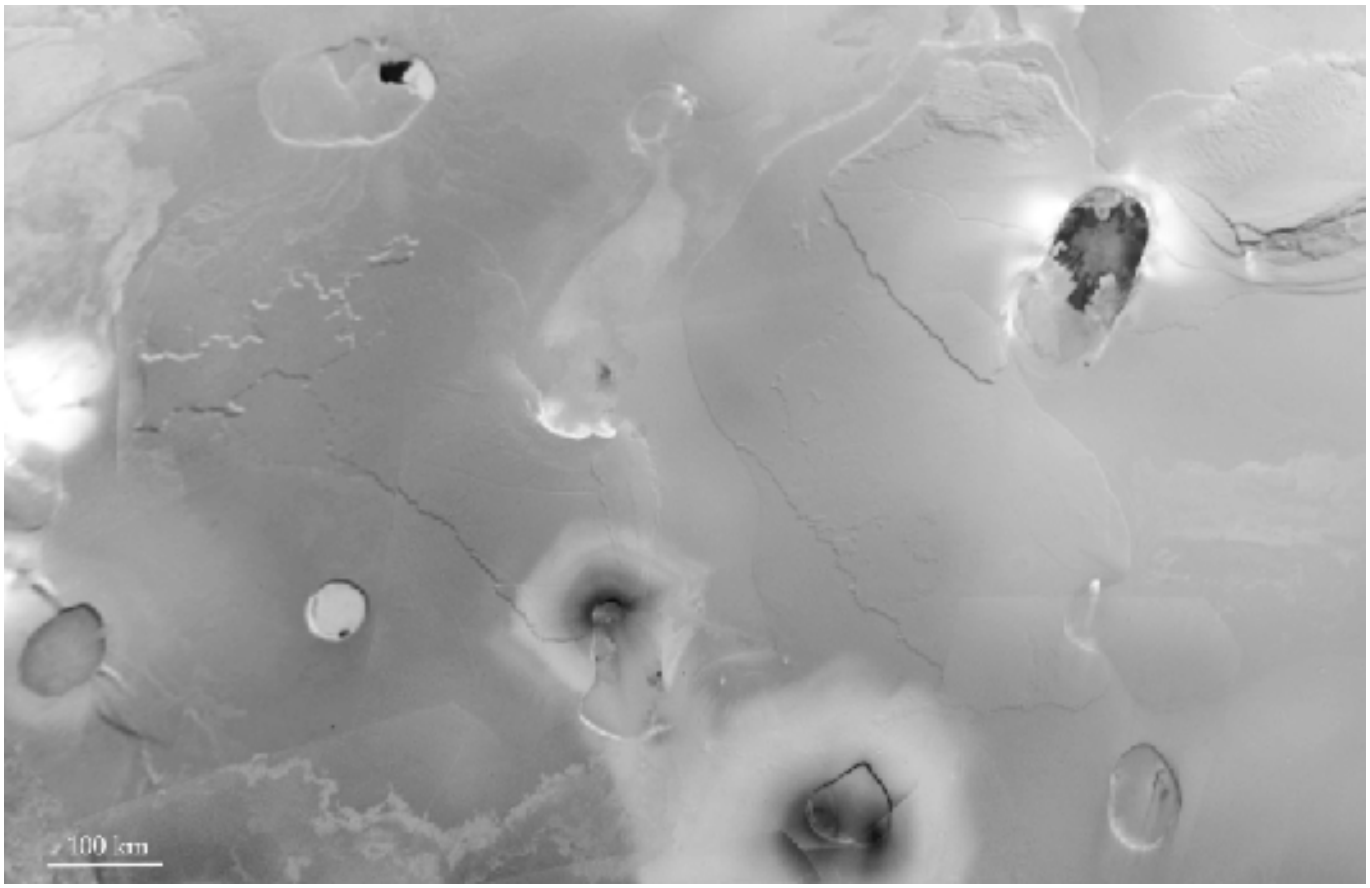

Figure 12. Mosaic of south polar region. Most of these paterae are large; for example, Kane Patera in the upper left of center is 144.4 km long axis. Many have round margins, compared with the paterae at low latitudes shown in Plate 1. Images taken by Voyager, <1 km pixel^{-1} resolution, ~330 W to 30 W, 85 S to 50 S, ~900 km across.

contaminated by other materials [*Schaber*, 1982; *Kargel et al.*, 1999] (Plate 1). Bright red material (the color of elemental short chain S_3 and S_4 polymorphs) diffusively streaks the floors and vents from the margins of the most active paterae (Plate 1) [*Schaber,* 1982; *McEwen et al.*, 1998a; *Geissler et al.*, 1999]. The diffuse material surrounding the margin of Monan Patera and a great portion of the patera floor south of the mountain (Figure 9) are both red, as are the deposits from the large plume Pele. This leads to the conclusion that S_2 gas is a component of the volatiles released upon eruption, confirmed at Pele [*Spencer et al.*, 2000]. The flows and coatings of various colors and textures intermix to produce mottled floors that are typical of recently active paterae on Io. The mottling, possibly a reflection of different flow ages and/or compositions and a hummocky surface morphology, conceals any floor fissures, vents, or preexisting patera walls, hiding evidence of multiple stages of collapse, if any multiple collapses have occurred (Figure 8).

3. Discussion and Interpretation

The implications of the characteristics of Ionian paterae described above are discussed in terms of the similarities and differences between paterae on Io and calderas on other planets. We then address the processes on Io that may produce the unique features we see.

3.1. Comparison With Terrestrial/Martian Basalt Shield Calderas

On Earth, low, broad shield volcanoes found on ocean islands such as Hawaii or the Galapagos Islands (Figure 5a) or in continental rift valley settings, such as the Snake River Plain, often have calderas at their summits. The morphology of these volcanoes is a direct result of the hot, fluid nature of the basalts that are incrementally erupted from vents on the summit and lower on the flanks. Calderas on these structures are characterized by arcuate margins, steep, nearly vertical walls, and multiple stages of collapse, evidenced by nesting of one caldera within another. The presence of low, shield-type features topped with calderas having these properties on Mars, such as on Olympus Mons, leads to the conclusion that these are also basalt shield

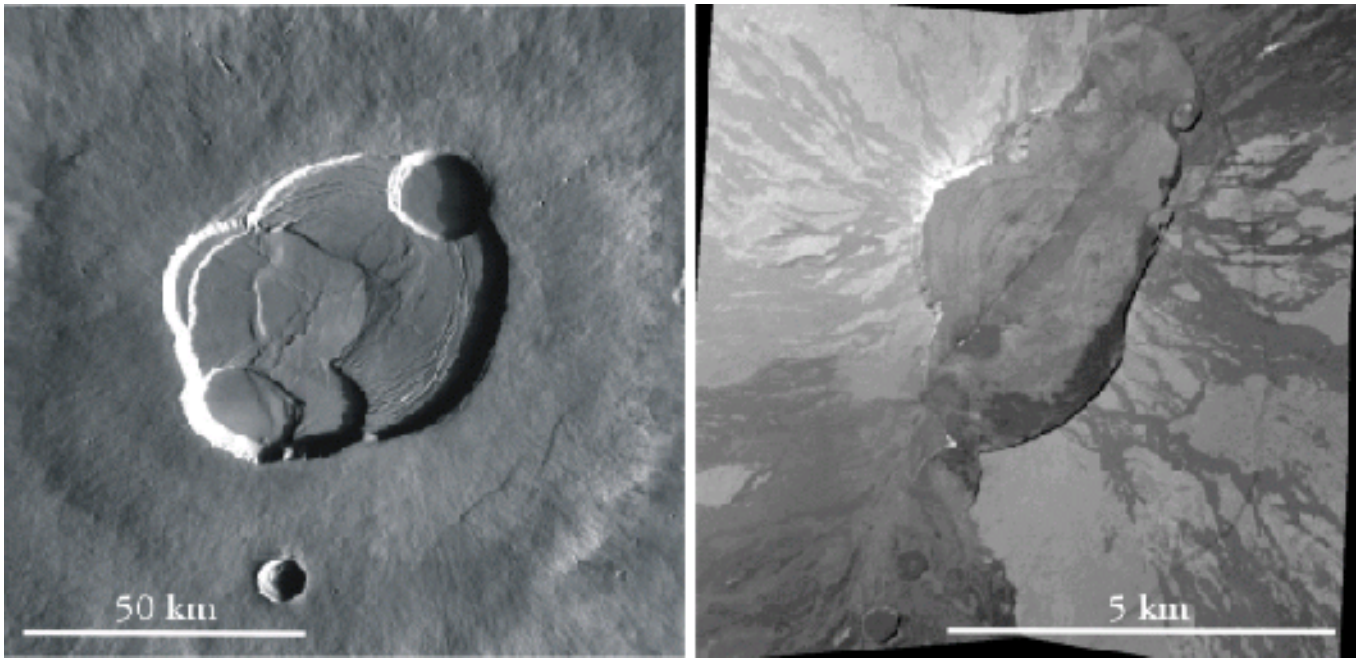

Figure 13. Caldera complexes atop (left) Olympus Mons and (right) Mauna Loa, Hawaii, are shown at different scales. Both complexes are elongate and exhibit several stages of collapse. Lavas flow downhill, away from the steep, arcuate, caldera walls. Olympus Mons image PIA 02982, courtesy of NASA/JPL/Caltech. Mauna Loa image from Compiled Volcanology Data Set 2 [Karas et al., 1994].

volcanoes and calderas (Figure 13). The type of caldera on Mars having this morphology is named for the above mentioned feature (Olympus-type), in contrast with the other (Arsia-type) [*Crumpler et al.*, 1996] that will be addressed along with calderas of Venus.

The size of volcanic shields found on Mars is much greater than that for terrestrial constructs [*Wood*, 1984]. For comparison, the largest volcanic structure on Earth is Mauna Loa volcano, Hawaii, which is on average 150 km in diameter at its base on the ocean floor and rises 10 km above that level, whereas Olympus Mons is ~550 km diameter at its base and rises 25 km above reference level. The mean diameter for 43 terrestrial basalt shield calderas is 6.6 km, the median is 5.3 km, and the peak in distribution occurs from 1 to 2 km (Table 1) [*Radebaugh*, 1999]. The mean diameter for all 37 Martian calderas is 47.7 km (close to the mean diameter for Ionian paterae of 41.0 km), their median is 39.0, and their mode is 20-25 km [*Crumpler et al.*, 1996].

The summit caldera complex atop Olympus Mons and the Mokuaweoweo caldera complex atop Mauna Loa are remarkably similar in morphology, although that atop Olympus Mons is almost 70 km in diameter, while Mokuaweoweo is only ~6 km in diameter *[Pike and Clow*, 1981]. Both have arcuate margins, steep, coherent walls and flat floors, and several features are nested within one another, due to multiple stages of collapse (Figure 13). Tvashtar Catena and Gish Bar Patera may also be nested caldera complexes. Tvashtar has two small paterae within one large one (Figure 11), while Gish Bar could conceivably be three separate nested calderas whose inner walls have been covered by varicolored lava flows (Figure 8).

At both Mauna Loa and Olympus Mons, lava flows radiate away from the calderas. It is possible that after the caldera collapsed, there was a period in eruptive history in which lava may have filled the caldera entirely then overtopped the walls and flowed out over the surface, a phenomenon that is rare on Earth but does occur in basalt shield calderas. Emakong Patera shows extensive flows emerging from its walls in all directions (Figure 6). If flows have filled the patera, overtopped the walls, and flowed out away for at least 50 km, this is a tremendous volume of lava to erupt (at least 1000 km^3 for a 500-m-deep patera). Extremely high heat flow and an efficient eruptive mechanism must exist in order to produce that amount of lava at the patera. This may also have happened at Prometheus, where at least three separate flows emerge from the straight southwest margin. An alternative explanation for these observations is that high-volume lava flows first emerged from a fissure vent, then the patera collapsed over the space from which the magma was evacuated. In either case, there is collapse due to the withdrawal of magma. It is difficult to determine the relative timing of eruptions and collapse, especially when using only postcaldera-formation remote sensing data.

3.2. Comparison With Terrestrial Ash Flow Calderas

Ash flow calderas are the largest volcanic features on Earth and are typically associated with the explosive eruption of copious amounts of silica-rich volcanic ash mixed with volatiles. These features generally do not have tall structural volcanic edifices associated with their initial formation, just broad aprons of deposits, justifying *Wood*'s [1984] description of these volcanoes as ash-flow shields. Although no large ash flow caldera has erupted in historical times, it is thought that these are features created by collapse over voids resulting from the eruption of magma from broad, shallow reservoirs. Examples of terrestrial ash flow calderas are Valles Caldera, New Mexico which is 24 km in diameter (Figure 5b); Long Valley Caldera in California, which is 21 km in diameter; and the Yellowstone Caldera complex, one caldera of which is 77 km in diameter, the largest known terrestrial caldera [*Pike and Clow*, 1981; *Spera and Crisp*, 1981].

Paterae on Io were initially compared with terrestrial ash flow calderas mainly because, in terms of size, only terrestrial ash flow calderas compare with Ionian paterae [*Carr et al.*, 1979; *Schaber*, 1982]. The mean diameter for 129 terrestrial ash flow calderas is 18.7 km, with a median of 15.4 km, and a peak in distribution at 12-13 km [*Radebaugh*, 1999; *Spera and Crisp,* 1981; *Best et al.*, 1989; *Lipman*, 1984; *Pike and Clow*, 1981], compared with a mean diameter of 41.0 km for Ionian paterae. An additional reason for the comparison is the lack of volcanic edifices on Io aside from paterae, with the rare exception of a few shallow shield-like features.

Io has undergone a significant amount of volcanic activity, and this activity could have greatly differentiated the body, concentrating low-density, high-silica materials, such as potassium and sodium silicates, in the crust, leaving higher-density, lower-silica content materials, such as dunite (pure olivine), in the mantle [*Keszthelyi and McEwen*, 1997]. There does not, however, appear to be any evidence for high-silica lava eruptions. In fact, from temperature, flow morphology, and limited compositional data the lavas appear to be mafic to ultramafic (Mg-rich) in composition [*McEwen et al.*, 1998b; *Keszthelyi et al.*, this issue].

Ash flow calderas are associated with resurgence, or postcaldera-forming eruptions. A large central resurgent dome as well as several smaller rhyolite domes are seen in Figure 5b of Valles Caldera; such features within ash flow calderas are typical. There is no evidence of this type of viscous dome-like resurgence in Io paterae [*Wood*, 1984]. However, their floors are the locations of deposition of new, dark, highly fluid, postpatera-forming lavas.

There are many terrestrial cases of bimodal volcanism, or silicic and mafic magma eruptions associated with the same volcanic system, such as at Yellowstone caldera. Highly silicic magmas can be obtained from mantle-derived magmas that ascend and partially melt crustal material: this partial melt ascends to shallow levels and forms batholithic masses or erupts pyroclastically. The mantle-derived mafic magma can later move upward through solidified silicic melt and erupt, resulting in layered or adjacent rhyolites and basalts [*Best*, 1982]. Iceland is a location where rhyolites and basalts are regularly found together at central volcanoes. In this region, magma evolution is probably brought about by partial melting of the basaltic volcanic pile, as it isostatically subsides deep into the crust [*Marsh et al.*, 1991].

Because of the low gravity and much lower atmospheric pressure, explosive, silicic eruptions on Io could produce deposits so fine-grained and widely dispersed that they would leave no well-defined deposits [*Wilson and Head*, 1983]. The silicic magma portion of caldera eruptions on Io would have to be restricted to plume-type, broad dispersal of material, though there is no evidence of deposits of felsic compositions to date.

One of the most intriguing possible eruption styles for Io is the mafic ash flow. A combination of mafic to ultramafic magmas, high volatile content (assumed because of the presence of large amounts of SO_2 on the surface and in plumes), and eruption into a 10^{-9} bar atmosphere could make explosive eruptions with mafic magmas common. It appears that the largest eruptions on Io do contain a significant explosive phase. That may have been the reason for the large, dark deposit (the size of the state of Arizona) that suddenly appeared at Pillan [*McEwen et al.*, 1998a] and the lava curtain at Tvashtar [*Wilson and Head*, this issue]. There is a substantial amount of diffuse, dark material that surrounds the most active paterae in the Camaxtli region (Plate 1); perhaps these are mafic pyroclastic deposits. Thus Io's paterae may be mafic ash flow calderas.

3.3. Comparison With Venus and Mars Arsia-Type Calderas

The surface of Venus is covered with large and small shield volcanoes, cones, domes, vast plains of lava flows, and other volcanic landforms. Calderas are found on Venus, both atop basalt-type shields and as large depressions lacking an appreciable edifice [*Head et al.*, 1992]. Large calderas on Venus not associated with an edifice are circular to elongate depressions with concentric fractures. These do not have steep, well-defined walls but do have a dark, central region indicating late, caldera-filling lavas [*Head et al.*, 1992]. There does not appear to be evidence for evolved, silica-rich magmas on Venus. An exception could be pancake domes, although these could be the result of mafic magma eruption in a high pressure environment [*Bridges*, 1995].

Arsia-type calderas of Mars are discussed here with calderas of Venus because there are similarities in their morphologies. Arsia-type calderas have wall morphologies

similar to those on Venus, in that the margins are not steep and abrupt, like the Mars Olympus-type, but are gently sloping and sag-like, with concentric fractures [*Crumpler et al.*, 1996]. Arsia-type calderas are larger than Olympus-type calderas, and the ratio of caldera diameter to shield diameter is greater than that for Olympus-type calderas. The best rationale for comparison of Ionian paterae with those of Venus and the Arsia-type on Mars again seems to be the similarity of their great sizes; for example, Sacajawea Patera is 200 km and Arsia Mons caldera is 115 km in diameter. There are 88 calderas measured on Venus (calderas only, having no associated shield); these range up to 200 km diameter, with a mean close to 68 km, and a median and peak in the distribution close to 70 km diameter [*Head et al.*, 1992; *Crumpler et al.*, 1996; *Radebaugh*, 1999] (Table 1). Data for Venusian calderas are incomplete and biased toward calderas with no constructional volcano beneath them. Once all calderas atop shields are included in the study, the mean and median for all Venus calderas may be smaller. The minimum diameter for Arsia-type calderas on Mars is 40 km, and the maximum is 145 km, so the mean is 80 km, greater than that for all Martian calderas of 47.7 km.

Ionian paterae do not generally have gently sloping, stepped walls and concentric fractures. In Plate 1, however, there are two features, one directly to the west, and the other to the southwest, of Camaxtli Patera that display this morphology. Many other paterae have ring-type fractures or steps that surround them; for example, Chaac Patera seems to be on a large plateau that steps down away from the patera on every side (Plate 1 and Figure 7).

The difference in appearance between typical Ionian paterae and those of Venus and Mars Arsia-type may indicate differences in lithospheric properties between the bodies. It may also suggest that most paterae on Io form in a single event or an abrupt collapse, leaving steep, straight walls, while Venusian and some Martian calderas have formed more gradually, leaving evidence of previous movements as circular fractures. Paterae/calderas of Io, Venus, and Mars show evidence of postcaldera lava flows that cover their floors, as do most terrestrial calderas.

3.4. Interior of Io

Paterae are critical to how Io removes her tremendous tidal energy. All of Io s measured heat flow emanates from ~100 hot spots, most of which occur in or adjacent to paterae [*Lopes-Gautier et al.*, 1999]. Analysis of the differences between paterae according to distribution on the body will enable us to better understand heat flow through Io s interior. High-latitude paterae, such as Tvashtar, Inti, and Hatchawa Paterae (Figures 11 and 12), all have steep walls and round to elliptical margins, and they usually have some active lava flows in their interior, without having their floors completely covered by dark lavas. They are larger than the mean, and their distribution is sparser. It may be that there is a different type of volcanism occurring at high latitudes, one that is marked by bursts of activity, then periods of quiescence, rather than the longer-lived, continuous, more effusive activity that seems to occur at low latitudes *[Lopes-Gautier et al.*, 1999; *Howell et al.*, this issue]. Perhaps this reflects a difference in lithospheric thickness [*McEwen et al.*, 2000]. If the lithosphere is thinner at low latitudes, then lava is closer to the surface and is more readily and frequently transferred upward through vents. It is possible, based on the differences in patera sizes at different longitudes, that there is also a thinner lithosphere at the sub-Jovian and anti-Jovian quarters of Io than at the leading and trailing quarters. A thicker lithosphere requires magma to be transported in large, buoyant batches or in smaller batches that feed large, sublithospheric magma chambers. Only when these chambers are periodically full might they produce high-volume, infrequent eruptions that leave partially vacant regions over which paterae form.

The association of tectonically formed mountains and volcanism has led to the hypothesis that mountain formation is partially controlled by mantle upwellings [*Turtle et al.*, this issue]. This model also predicts the formation of preferred magma conduits along the fractures bounding mountains. It appears that in many paterae, lava erupts from the base of the patera walls, likely because the magma moves upward along deep fractures bounding paterae [*Keszthelyi et al.*, this issue]. While this model is still being tested, it begins to produce a picture that links the volcanism and tectonics on Io with the dynamics of its interior.

The asthenospheric model for tidal heating in Io predicts that there should be centers of convection in the asthenosphere such that there is upwelling and downwelling separated by several hundred kilometers, rather than larger-scale convection resulting in a few widely spaced mantle plumes [*Tackley et al.*, 2001]. In addition, asthenospheric heat flow patterns predicted by *Ross et al.* [1990] show greatest thermal upwellings at the sub-Jovian and anti-Jovian points, with several smaller heat flow highs between these points at low latitudes. The newly catalogued Ionian paterae show a distribution with latitude that is similar to the distribution of persistent hotspots discussed by *Lopes-Gautier et al.* [1999] (Figure 3). These latitudinal distributions, separations between paterae, and longitudinal clustering are all consistent with the idea that tidal heating is concentrated in the upper mantle. In addition, *Tackley et al.* [2001] note that their assessment of the distribution of volcanoes on Io (similar to the distribution of paterae [see also *Schenk et al.*, this issue]) confirms the asthenospheric heating pattern.

It is curious that the longitudinal peaks in patera number do not exactly coincide with the sub-Jovian and anti-Jovian points. The variation in longitudinal patera distribution is significant; the peak values are double the low values, even for data normalized to coverage (Figure 4).

There is a small region from 200 W to 270 W, 30 N to 60 N at 3.2 km pixel^{-1}, yet at higher resolution (1-2 km pixel^{-1}) this region would not reveal double the number of paterae that have already been measured there. Thus reasons for the longitudinal distribution should be considered. Since tidal massaging is most dramatic along Io s Jupiter-pointing axis (longitude 0 and 180), it is plausible that more magmas could be generated near the sub-Jovian and anti-Jovian regions [*Ross et al.*, 1990; *Lopes-Gautier et al.*, 1999]. With more lava generation and translation through the lithosphere, more magma chambers and lava eruptions occur, leading to the formation of more paterae. Yet the paterae cluster around 330 W and 150 W longitude, offset eastward by 30 from the Jupiter-pointing axis. An inventory of possible volcanic centers (defined as the point source from which volcanic resurfacing events originate, including paterae) by *Schenk et al.* [this issue] reveals similar results; there are peaks in distribution at 325 W and 165 W longitudes. Perhaps tidal massaging is tied with some other interior magma creation or diffusion process that shifts the distribution of paterae/volcanic centers. Io could also have undergone or be undergoing an epoch of nonsynchronous rotation [*Greenberg and Weidenschilling*, 1984; *Gaskell et al.*, 1988; *Tackley et al.*, 2001], so that the most active hemispheres lead the current 0 and 180 points by 30 . If the rate of nonsynchronous rotation could be determined, this would provide a constraint for time scales of volcanic processes [*Milazzo, et al.*, 2001].

3.5. Modes of Caldera Formation: Problems for Ionian Paterae

Several terrestrial caldera formation models were created based on volcano/caldera morphologies, compositions, behaviors over time, and local conditions surrounding different caldera types. Paterae on Io are compared with these models, and we have created some additional models to suit the unique environment of Io.

1. Flank eruptions lead to caldera formation atop terrestrial/Martian basalt shield volcanoes through subsequent collapse of overlying material into the evacuated magma chamber [*Francis*, 1993] (Figure 14a). An example of this exists in the current eruption of Kilauea volcano on Hawaii; most magma emerges through vents on the flanks. Previous similar eruptions led to the collapse of the Kilauea caldera. Shields on Io appear to be rare; however, there may be a few examples of downflank eruptions on Io. For example, a dark channel apparently emerges not directly from Emakong s patera wall but several tens of kilometers away. A long, lava tube-like channel may have formed as a flank eruption from Culann Patera, and a wide dark flow begins several kilometers downslope from Susanoo Patera.

2. Piston-like collapse over an evacuated shallow silicic magma chamber is thought to result in formation of a terrestrial ash flow caldera, the dimensions of which are similar to the magma chamber volume before eruption [*Smith and Bailey*, 1968; *Smith*, 1979; *Lipman*, 1997] (Figure 14b). Variations on the piston-like collapse model are piecemeal, trapdoor, and even funnel-like collapse, all based on the need for downward movement of large amounts of crust into partially empty magma chambers [*Lipman*, 1997]. These large magma chambers are probably able to form from coalesced pods of magma at such shallow depths because of the density contrast in the lithosphere between hot, buoyant, silicic magma and cool, more mafic country rock. Magmas on Io are more mafic than those described here, and on Earth, mafic magmas do not typically coalesce into large reservoirs at shallow depths. On Io, however, depths of magma reservoirs may be controlled mostly by pore space volume in country rock. For a pore space volume of ~30% the neutral buoyancy zone, and depth to magma reservoir, is ~30 km. This zone becomes increasingly

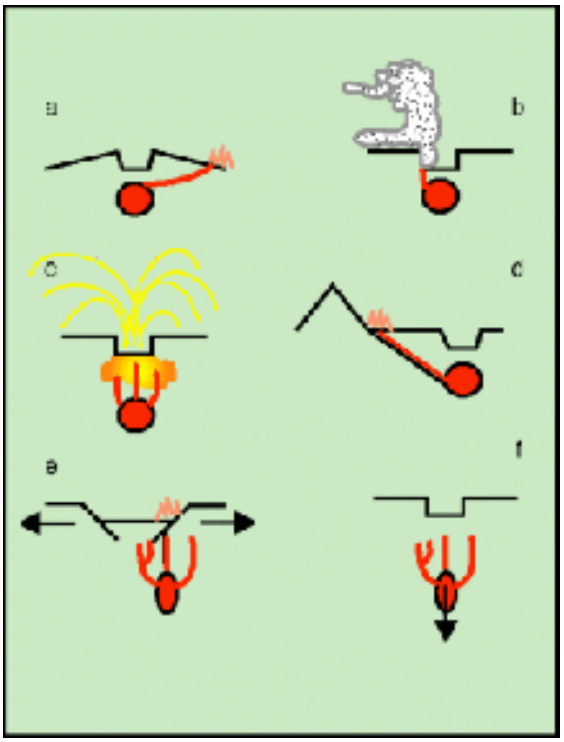

Figure 14. Models for possible patera formation on Io. (a) Flank eruption of lava from a basalt shield volcano leads to caldera formation. (b) Piston-like collapse occurs after evacuation of a silicic magma chamber [from Lipman, 1997]. (c) Interaction of lava with volatiles in the crust leads to plume eruptions and collapse over empty region, (d) paterae form with mountains, leading to magma movement along faults. (e) Large pull-apart basins may result from tectonic activity; their floors are then covered with lava. (f) Dense intrusive rocks may founder into the magma source region, leading to surface collapse [from Walker, 1988].

shallow for smaller fractions of pore space [*Leone and Wilson*, this issue].

3. Explosive plume eruptions and subsequent deposition of the ubiquitous frost (mostly SO_2) are caused by the release of crustal or magmatic volatiles. Dikes of mafic magma may rise through the crust from a deeper reservoir and then make contact with frozen volatiles, such as SO_2, in the crust, leading to a plume eruption and subsequent collapse of the evacuated subsurface (Figure 14c). Perhaps shallow magma chambers (present because of pore space volume <30%) also interact with crustal volatiles, or they reach a shallow enough depth that water attempts to exsolve from the magma, leading to the explosive eruption of mafic pyroclastics [*Leone and Wilson*, this issue].

4. Tectonic influence in patera formation is important to consider because of the irregularity in shape of many Ionian paterae. Since mountains and plateaus are often associated with paterae [*Turtle et al.*, this issue; *Jaeger et al.*, 2001], we conclude that some paterae may form in concert with the formation or evolution of mountains. It is difficult to determine, by observations only, the relative ages of certain paterae and associated mountains. However, judging by the patera wall morphologies, it is clear that movement of the crust along mountain-associated faults was still active during patera formation. A recently observed lava fissure eruption within Tvashtar Catena occurred near a patera wall, several tens of kilometers from the base of a mountain, and was probably created by magma rising along complicated local faults (Figure 14d). Eruptions like this could lead to evacuation of a local magma chamber and caldera collapse.

5. Some paterae appear to have formed as graben-type features, by the pulling apart of crustal material, such as at Hi iaka or Monan Patera [*Jaeger et al.*, 2001]. Fractures in the crust from the tectonic activity create magma conduits up which magma travels and then erupts onto floors of newly formed grabens, pull-apart basins, or depressions from crustal subsidence (Figure 14e).

6. Dense magma or solidified intrusive material that has accumulated in the crust can sink back down into the mantle, creating a void over which overlying crustal material collapses [*Walker*, 1988]. Dikes emerge from a deeper magma source region to feed eruptions, then as this system cools and solidifies, its density increases. In order for this material to sink, the upper mantle beneath it must be less dense, or the intrusive material would never founder. This scenario is possible if we consider the upper mantle to be a magma ocean (either locally or on a global scale), in which the partially molten mantle material is less dense than solidified or more mafic magma [*Keszthelyi et al.*, 1999] (Figure 14f).

There is good evidence for the occurrence of flank eruptions on Io, which makes the patera formation model typical of basalt shield calderas viable. Many of the paterae, however, rest on flat plains, not large shields. Their great sizes make the ash flow caldera formation model attractive, with collapse of a large area of crust. Paterae on Io vary widely in size, association with other paterae or mountains, and in regularity of margins, so it is possible that no one model adequately describes the formation of all paterae on Io. Perhaps it is necessary to consider a combination of all of them in order to explain the unique features seen on Io.

4. Summary and Conclusions

Paterae on Io are intriguing because they exhibit some characteristics common to various types of calderas in the solar system; yet there are significant aspects of these features that are unique to Io. Because of their morphologies and erupted products, perhaps we can conclude that paterae on Io are a unique hybrid of basalt shield and mafic ash flow caldera.

Paterae on Io are affected by the tectonics of the tidally stretched body. Their margins are often irregular or straight, and many are found adjacent to mountains or plateaus. Some paterae appear to have formed by the rifting apart of the crust and subsequent covering of the paterae floors by lavas. Of 417 paterae measured at <3.2 km pixel^{-1} resolution by Galileo and Voyager (80% of Io's surface), 43% have irregular or straight margins.

The mean diameter for all paterae on Io is 41.0 km, smaller than the mean diameters for Martian and Venusian calderas of 47.7 and 68 km, respectively, while the mean diameter is 6.6 km for terrestrial basalt shield calderas and 18.7 km for ash-flow calderas. There is a bias toward paterae forming within an equatorial band from +25° to -25° latitude, and paterae also tend to cluster around 330° W and 150° W longitudes. These concentrations probably exist partly because tidal distortion is greatest along the Jupiter-pointing axis of Io (0° and 180° W longitude). Asymmetries in tidal heating, explained by the asthenospheric model, coupled with possible nonsynchronous rotation, may be manifest in these nonuniform patera distributions and varying styles of volcanism. At the midlatitudes are many long-lived, effusive hot spots, while near the poles, there are larger, more widely spaced paterae associated with episodic volcanism.

We are still in the early stages of our understanding of paterae on Io. These features may follow formation mechanisms considered for planetary calderas, yet major elements of patera formation on Io remain unanswered. Ionian paterae and planetary calderas are directly tied to the volcanic and tectonic processes immediately beneath them and thus form windows to the interiors of bodies. Further analysis of these new comparisons of calderas on Earth, Mars, and Venus with paterae on Io will lead to a better understanding of patera formation and evolution and of the magmatic processes in planetary interiors.

Acknowledgments. The authors appreciate the assistance of Paul Geissler, Eric H Christiansen, Frank Chuang, David Williams, and especially Ellen Stofan and Steven Anderson for their ideas, reviews, and comments. The work of Paul Lucey and Sheenan Morrison was key in facilitating the review process and is appreciated. Most images were processed at the Planetary Image Research Laboratory, University of Arizona, unless otherwise stated. Thanks also go to Galileo spacecraft for her persistence. This research supported by the Galileo project.

References

Best, M. G., *Igneous and Metamorphic Petrology*, 630 pp., Blackwell Sci., Malden, Mass., 1982.

Best, M. G., E. H Christiansen, and R. H. Blank Jr., Oligocene caldera complex and calc-calkaline tuffs and lavas of the Indian Peak volcanic field, Nevada and Utah, *Geol. Soc. Am. Bull.*, *101*, 1076-1090, 1989.

Bridges, N. T., Submarine analogs to Venusian pancake domes, *Geophys. Res. Lett.*, *22*, 2781-2784, 1995.

Carr, M. H., and G. D. Clow, The structure of the Ionian lithosphere, *NASA Tech. Memo.*, *TM-86246*, 11-13, 1984.

Carr, M. H., H. Masursky, R. G. Strom, and R. J. Terrile, Volcanic features of Io, *Nature*, *280*, 729-733, 1979.

Crumpler, L. S., J. W. Head, and J. C. Aubele, Calderas on Mars: Characteristics, structure, and associated flank deformation, in *Volcano Instability on the Earth and Other Planets* edited by W J. McGuire, A. P. Jones, and J. Neuberg, *Geol. Soc. Spec. Pub., 110*, 307-308, 1996.

Davies, A. G., L. P. Keszthelyi, D. A. Williams, C. B. Phillips, A. S. McEwen, R. M. C. Lopes-Gautier, W. D. Smythe, L. W. Kamp, L. A. Soderblom, and R. W. Carlson, Thermal signature, eruption style, and eruption evolution at Pele and Pillan on Io, *J. Geophys. Res.*, this issue.

Francis, P. W., *Volcanoes: A Planetary Perspective*, 443 pp., Oxford Univ. Press, New York 1993.

Gaskell, R. W., S. P. Synnott, A. S. McEwen, and G. G. Schaber, Large-scale topography of Io: Implications for internal structure and heat transfer, *Geophys. Res. Lett.*, *15*, 581-584, 1988.

Geissler, P. E., A. S. McEwen, L. Keszthelyi, R. Lopes-Gautier, J. Granahan, and D. P. Simonelli, Global color variations on Io, *Icarus*, *140*, 265-282, 1999.

Greenburg, R., and S. J. Weidenschilling, How fast do Galilean satellites spin?, *Icarus*, *58*, 186-196, 1984.

Head, J. W., L. S. Crumpler, and J. C. Aubele, Venus volcanism: Classification of volcanic features and structures, associations, and global distributions from Magellan data, *J. Geophys. Res.*, *97*, 13,153-13,197, 1992.

Howell, R. R., et al., Ground-based observations of volcanism on Io in 1999 and early 2000, *J. Geophys. Res.*, this issue.

Jackson, J.A., (Ed.), *Glossary of Geology*, 4th ed., 769 pp., Am. Geophys. Instit., Alexandria, Va., 1997.

Jaeger, W., E. P. Turtle, L. P. Keszthelyi, and A. S. McEwen, Orogenic tectonism on Io, *Lunar Planet. Sci. Conf.*, *XXXII*, abstract, 2045, 2001.

Johnson, T. V., and L. A. Soderblom, Volcanic eruptions on Io: Implications for surface evolution and mass loss, in *Satellites of Jupiter*, edited by D. Morrison, pp. 634-646, Univ. of Ariz. Press, Tucson, 1982.

Kargel, J. S., P. Delmelle, and D. B. Nash, Volcanogenic sulfur on Earth and Io: Composition and spectroscopy, *Icarus*, *142*, 249-280, 1999.

Keszthelyi, L., and A. S. McEwen, Magmatic differentiation of Io, *Icarus*, *130*, 437-448, 1997.

Keszthelyi L., A. S. McEwen, and G. J. Taylor, Revisiting the hypothesis of a mushy global magma ocean in Io, *Icarus*, *141*, 415-419, 1999.

Keszthelyi, L., A. S. McEwen, C. Phillips, M. Milazzo, P. Geissler, D. Williams, E. P. Turtle, J. Radebaugh, D. Simonelli, and the Galileo SSI Team, Imaging of volcanic activity on Jupiter s moon Io by Galileo during Galileo Europa Mission and Galileo Millenium Mission, *J. Geophys. Res.*, this issue.

Leone, G., and L. Wilson, Density structure of Io and the migration of magma through its lithosphere, *J. Geophys. Res.*, this issue.

Lipman, P. W., Subsidence of ash-flow calderas: relation to caldera size and magma-chamber geometry, *Bull. Volcanol.*, *59*, 198-218, 1997.

Lipman, P. W., The roots of ash flow calderas in western North America: Windows into the tops of granitic batholiths, *J. Geophys. Res.*, *89*, 8801-8841, 1984.

Lopes-Gautier, R., et al., A close-up look at Io from Galileo s near-infrared mapping spectrometer, Science, 288, 1201-1204, 2000.

Lopes-Gautier, R., et al., Active volcanism on Io: Global distribution and variations in activity, *Icarus*, *140*, 243-264, 1999.

Marsh, B. D., B. Gunnarsson, R. Congdon, and R. Carmody, Hawaiian basalt and Icelandic rhyolite: Indicators of differentiation and partial melting, *Geol. Rundsh.*, *80*(2), 481-510, 1991.

McEwen, A. S., D. L. Matson, T. V. Johnson, and L. A. Soderblom, Volcanic hot spots on Io: Correlation with low-albedo calderas, *J. Geophys. Res.*, *90*, 12,345-12,379, 1985.

McEwen, A. S., D. P. Simonelli, D. R. Senske, K. P. Klaasen, L. Keszthelyi, T. V. Johnson, P. E. Geissler, M. H. Carr, M. J. S. Belton, High-temperature hot spots on Io as seen by the Galileo solid-state imaging (SSI) experiment, *Geophys. Res. Lett.*, *24*, 2443-2446, 1997.

McEwen, A. S., et al., Active volcanism on Io as seen by Galileo SSI, *Icarus*, *135*, 181-219, 1998a.

McEwen, A. S., et al., High-temperature silicate volcanism on Jupiter s moon Io, *Science*, *281*, 87-90, 1998b.

McEwen, A. S., et al., Galileo at Io: Results from high-resolution imaging, *Science*, *288*, 1193-1198, 2000.

Milazzo, M. P., P. E. Geissler, R. Greenberg, L. P. Keszthelyi, A. S. McEwen, J. Radebaugh, and E. P. Turtle, Does Io rotate non-synchronously? *Lunar Planet. Sci. Conf.*, *XXXII*, Abstract, 2089, 2001.

Moore, J. M., A. S. McEwen, E. F. Albin, and R. Greeley, Topographic evidence for shield volcanism on Io, *Icarus*, *67*, 181-183, 1986.

Phillips, C. B., Voyager and Galileo SSI views of volcanic resurfacing on Io and the search for geologic activity on Europa, Ph.D. thesis, Univ. of Ariz., Tucson, 2000.

Pike, R. J., and G. D. Clow, Revised classification of terrestrial volcanoes and catalog of topographic dimensions, with new results on edifice volume, *U.S. Geol. Surv. Open File Rep.*, *81-1038*, 40 pp., 1981.

Radebaugh, J., Terrestrial pluton and planetary caldera sizes: Implications for the origin of calderas, M.S. thesis, Brigham Young Univ., Provo, Utah, 1999.

Ross, M. N., G. Schubert, T. Spohn, and R. W. Gaskell, Internal structure of Io and the global distributions of its topography, *Icarus*, *85*, 309-325, 1990.

Schaber, G. G., The geology of Io, in *Satellites of Jupiter*, edited by D. Morrison, pp. 556-597, Univ. of Ariz. Press, Tucson, 1982.

Schenk, P., H. Hargitai, R. Wilson, A. McEwen, and P. Thomas, The mountains of Io: Global and geological perspectives from Voyager and Galileo, *J. Geophys. Res.*, this issue.

Smith, R. L., Ash-flow magmatism, *Geol. Soc. Am. Spec. Pap.*, *180*, 343-365, 1979.

Smith, R. L., and R. A. Bailey, Resurgent cauldrons, *Geol. Soc. Am. Mem.*, *116*, 83-104, 1968.

Spencer, J. R., K. L. Jessup, M. A. McGrath, G. E. Ballester, and R. Yelle, Discovery of gaseous S_2 in Io s Pele plume, *Science*, *288*, 1208-1210, 2000.

Spera, F. J., and J. A. Crisp, Eruption volume, periodicity, and caldera area: Relationships and inferences on development of compositional zonation in silicic magma chambers, *J. Volcanol. Geotherm. Res.*, *11*, 169-187, 1981.

Tackley, P. J., G. Schubert, G. A. Glatzmaier, P. Schenk, J. T. Ratcliff, and J. P. Matas, Three-dimensional simulations of mantle convection in Io, *Icarus*, *149*, 79-93, 2001.

Turtle, E. P., et al., Mountains on Io: High-resolution Galileo observations, initial interpretations, and formation models, *J. Geophys. Res.*, this issue.

Walker, G. P. L., Three Hawaiian calderas: An origin through loading by shallow intrusions?, *J. Geophys. Res.*, *93*, 14,773-14,784, 1988.

Williams, D. A., R. Greeley, R. Lopes-Gautier, and A. Davies, Evaluation of sulfur flow emplacement on Io from Galileo data and numerical modeling, *J. Geophys. Res.*, this issue.

Williams, H., Calderas and their origin, *Univ. Calif. Pub. Geol. Sci.*, *25*(6), 239-346, 1941.

Wilson, L., and J. W. Head, A comparison of volcanic eruption processes on Earth, Moon, Mars, Io, and Venus, *Nature*, *302*, 663-669, 1983.

Wilson, L., and J. W. Head III, Lava fountains from the 1999 Tvashtar Catena fissure eruption on Io: Implications for dike emplacement mechanisms, eruption rates, and crustal structure, *J. Geophys. Res.*, this issue.

Wood, C. A., Calderas: A planetary perspective, *J. Geophys. Res.*, *89*, 8391-8406, 1984.

W. Jaeger, L. P. Keszthelyi, A. S. McEwen, M. Milazzo, J. Radebaugh, and E. P. Turtle, Lunar and Planetary Laboratory, 1629 E. University Blvd., Tucson, AZ 85721-0092. (jaeger@LPL.arizona.edu, lpk@pirl.LPL.arizona.edu, mcewen@pirl.LPL.arizona.edu, mmilazzo@pirl.LPL.-arizona.edu, jani@LPL.arizona.edu, turtle@pirl.LPL.-arizona.edu)

(Received October 2, 2000, revised March 14, 2001, accepted April 27, 2001.)